Vision Res. Vol. 17, pp. 1075 to 1082. Pergamon Press 1977. Printed in Great Britain.

ORTHOGONAL COMBINATION OF THE THREE VISUAL CHANNELS

CARL R. INGLING, JR. and BRIAN HUONG-PENG TSOU

Institute for Research in Vision and Department of Biophysics, Ohio State University, 1314 Kinnear Road, Columbus, OH 43212, U.S.A.

(*Received* 12 *January* 1976; *in revised form* 14 *February* 1977)

Abstract—The responses of three cone types are differenced and summed by receptive fields reported in electrophysiological studies to form two opponent, or chromatic, and one luminance channel. The responses of these three transformed channels are orthogonally combined at a detector. The spectral sensitivity of the transformed channels is a function of intensity and adaptation; transformation equations are given for threshold and suprathreshold. The channel responses, represented as distance along axes in a vector space, have different temporal and spatial properties, depending upon the characteristics of the receptive fields associated with each axis. Spectral sensitivities, Stiles's π_5, Guth's data on threshold subadditivity, saturation discrimination and hue discrimination are modeled in the space.

INTRODUCTION

Guth and Lodge (1973) recently described a vector model for threshold color vision. In searching for a simple, quantitative representation of those discrimination functions which include wavelength as a significant variable, we also were led, by analogy with color-space diagrams and by the success of Kaiser, Herzberg and Boynton's (1971) orthogonal combination of channels, to try a Euclidean space (Ingling, Tsou and Nosek, 1973). Although our starting point was different, the two models are coincidentally similar, and in many instances make the same predictions.

THE VECTOR MODEL

Figure 1 illustrates the physiological properties of the vector space. This space summarizes much data and theory about which there is general, although not universal, agreement. The receptive fields shown in the X–Z, or opponent-color plane, are both chromatically and spatially opponent. They signal the difference between quantum absorptions in, say, the L and M pigments, and also signal information about spatial luminance or brightness contrasts. The receptive fields on the Y, or luminance, axis are color-blind because the spectral sensitivity of the surround and center are the same. The receptive field organizations of this diagram are those reported in the electrophysiological literature, although usually a few per cent of the cells are not of these two general types. For example, the cells on the luminance axis are presumably DeValois, Abramov and Jacob's (1966) broad-band, Wiesel and Hubel's (1966) Type III, and Gouras's (1968) phasic cells; those in the chromatic plane are DeValois *et al.*'s narrow band, Wiesel and Hubel's Type I, and Gouras's tonic cells. The organization of the space represents the opponent-colors transformation; it models the quantities in the sum and difference channels, and gives a rule for combining the three receptive field outputs as resultants in a vector space. Figure 2 shows the spectral sensitivities of the receptor stage, the opponent stage, and the detector which orthogonally combines the opponent stage outputs. Distance in the space, symbolized by S, is given by the formula

$$S^2 = Q^2\,[(r-g)^2 + (y-b)^2 + V_\lambda^2], \qquad (1)$$

and represents visual response. Q is light intensity, a scalar multiplier. Thus the formula is of the form Response = Intensity × Sensitivity.

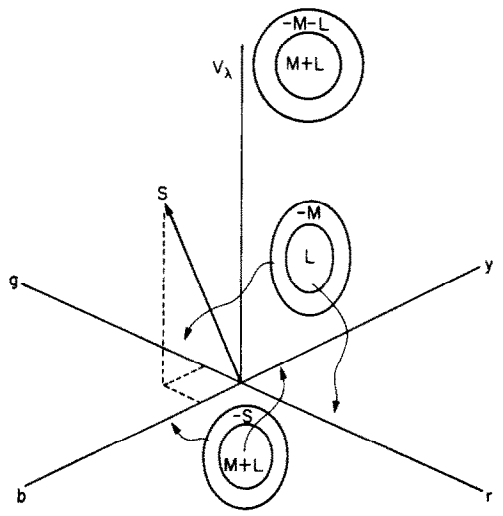

Fig. 1. Illustration of the vector space, showing the receptive fields which compute the chromatic, or opponent, and the luminance signals. The outputs of the three receptive fields are combined orthogonally to produce visual response, S.

THE TRANSFORMATION EQUATIONS

If the opponent curves are linear combinations of the fundamental sensitivities, the shape chosen for the fundamentals is unimportant; any linear combination of the color-matching functions will do. However, if non-linearities are introduced in the opponent transformation, the precise form of the fundamentals becomes important. We have used two sets of fundamentals extensively: Vos and Walraven's (1971) RGB and Smith and Pokorny's (personal communication, Table 1) LMS. Transformations to the

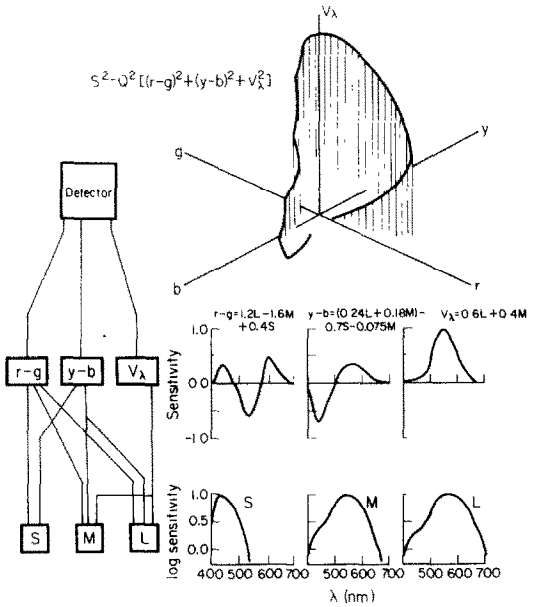

Fig. 2. Left: the receptor, differencing and summing, and detector stages. Right: the spectral sensitivity of the channels at each stage. The spectral sensitivity of the detector is plotted as a locus in the color space which is an orthogonal combination of the sensitivities of the previous stage. Detector and opponent-stage sensitivities are shown for the suprathreshold form.

threshold form of the opponent curves for the LMS fundamentals are (see Fig. 3):

$$r\text{–}g = 1.2L - 1.6M \tag{2a}$$

$$y\text{–}b = K_1(0.24L + 0.18M) - K_2(0.70S) - 0.075\,M \tag{2b}$$

$$K_1 = 0.20 \qquad K_2 = 0.06$$

$$V_\lambda = 0.6L + 0.4M. \tag{2c}$$

The suprathreshold forms are:

$$r\text{–}g = 1.2L - 1.6M + 0.4S \tag{3a}$$

$$y\text{–}b = K_1(0.24L + 0.18M) - K_2(0.7S) - 0.075M \tag{3b}$$

$$K_1 = K_2 = 1$$

$$V_\lambda = 0.6L + 0.4M. \tag{3c}$$

The relationship of the threshold to the suprathreshold forms is discussed by Ingling (1977). It may prove possible to reduce these equations to a single set by introducing intensity and adaptation-dependent operators into the above equations as follows:

$$r\text{–}g = -(-1.2L + 1.6M\,\theta\,0.4S) \tag{4a}$$

$$y\text{–}b = K_1(0.24L + 0.18M) - K_2(0.7S) - 0.075M. \tag{4b}$$

The symbol θ indicates a special subtraction (see above reference). Once the adaptation is specified, the above equations produce opponent curves of both the threshold and suprathreshold form. However, for the computational purposes of this report the discrete threshold–suprathreshold equations are used. Further, only the functions obtained using the Smith and Pokorny LMS sensitivities will be shown. Vos and Walraven's RGB yield similar forms; a version is given in the Appendix.

SPECTRAL SENSITIVITY

We have outlined a model for computing visual response, S. The model orthogonally combines the output of three channels, two opponent and one luminance, weighted by a scalar intensity, Q. Most of the discrimination functions to be derived using this model require computing a spectral sensitivity under a given set of conditions. These conditions are simulated in the response space by modifying with coefficients the terms which contribute to S. Although inspection of the conditions under which, say, a π mechanism or a saturation discrimination function is measured suggest *a priori* adjustments to the equation, numerical values for the coefficients must be obtained by curve fitting. Thus, while 1000-td white-light adaptations depress the sensitivity of the V_λ channel term relative to the chromatic channels, exactly how much is an empirical question.

For a linear system, either the response to unit radiance, or the reciprocal of the radiance required for criterion response as a function of wavelength, gives the spectral sensitivity. Because equation (1) is linear, given the values for r,g,y,b, and V_λ for each wavelength, either definition can be used to calculate the spectral sensitivity. For the former definition, Q is fixed and the quantity S is calculated for each wavelength. However, for practical reasons involving computations not reported here we use the latter defini-

Table 1. Smith and Pokorny's fundamental spectral sensitivities for the human photopigments at the cornea (personal communication)

	L	M	S
400	0.547-02	0.552-02	0.908-01
410	0.141-01	0.150-01	0.262+00
420	0.210-01	0.244-01	0.644+00
430	0.302-01	0.388-01	0.931+00
440	0.385-01	0.548-01	1.000+00
450	0.407-01	0.677-01	0.910+00
460	0.459-01	0.830-01	0.682+00
470	0.713-01	0.125+00	0.520+00
480	0.995-01	0.169+00	0.352+00
490	0.125+00	0.209+00	0.212+00
500	0.225+00	0.350+00	0.134+00
510	0.412+00	0.581+00	0.689-01
520	0.611+00	0.791+00	0.333-01
530	0.771+00	0.936+00	0.126-01
540	0.877+00	1.000+00	0.456-02
550	0.942+00	0.990+00	0.177-02
560	0.988+00	0.926+00	0.625-03
570	1.000+00	0.809+00	0.230-03
580	0.967+00	0.653+00	0.873-04
590	0.896+00	0.478+00	0.342-04
600	0.797+00	0.319+00	0.139-04
610	0.666+00	0.194+00	0.578-05
620	0.501+00	0.111+00	0.248-05
630	0.381+00	0.585-01	0.109-05
640	0.257+00	0.297-01	0.494-06
650	0.159+00	0.144-01	0.229-06
660	0.916-01	0.703-02	0.109-06
670	0.483-01	0.335-02	0.526-07
680	0.257-01	0.166-02	0.261-07
690	0.124-01	0.767-03	0.132-07
700	0.626-02	0.307-03	0.681-08

Sensitivities are normalized to 1.0 at the wavelength of maximum sensitivity: S = short-wavelength, M = middle-wavelength, L = long-wavelength sensitivities. The S pigment has been extrapolated by using the V_λ' slope on a frequency abscissa.

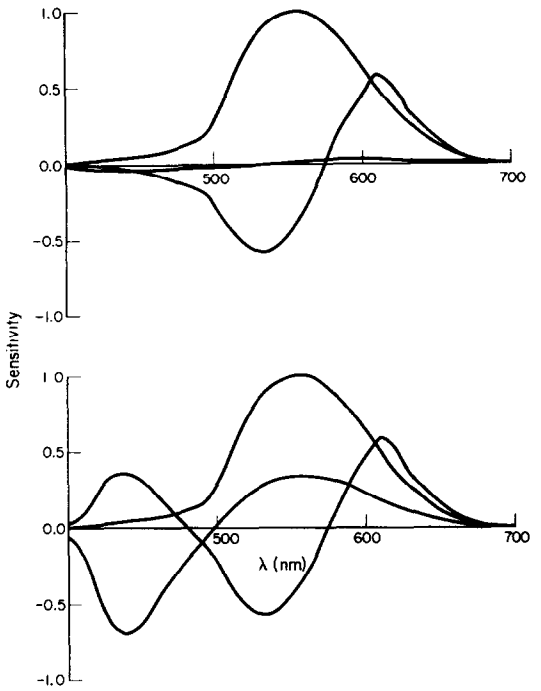

Fig. 3. The spectral sensitivity of the opponent and luminance channels at threshold (top) and for light-adapted suprathreshold (bottom) as given by equations (2) and (3).

tion, for which the relative spectral sensitivity of the detector is obtained by setting S to a constant and solving for $1/Q$ at each wavelength. Even if equation (1) is modified by introducing nonlinearities, this latter definition yields the correct spectral sensitivity.

Figure 4 shows log $1/Q$ for threshold [from equations (1) and (2)] compared to the dark-adapted foveal spectral sensitivity curve of Hsia and Graham (1957). Figure 5 shows log $1/Q$ for suprathreshold [equations (1) and (3)] for two cases.

The upper dotted curve is for equation (1) with no differential weights. This curve is only of theoretical interest, because although it supposedly is the spectral sensitivity for white-light adaptation, such adaptation necessarily

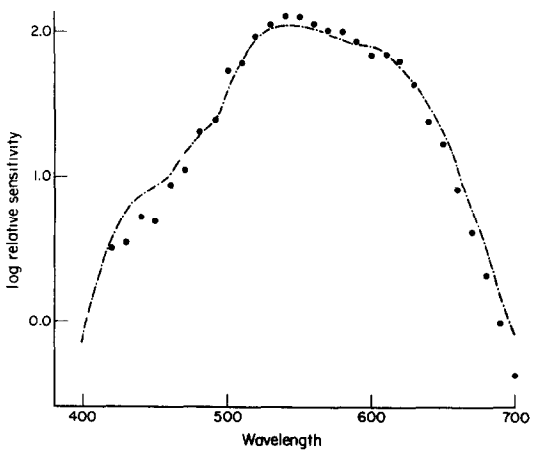

Fig. 4. The spectral sensitivity of the detector at threshold, from equations (2), compared to Hsia and Graham's (1957) average of seven observers.

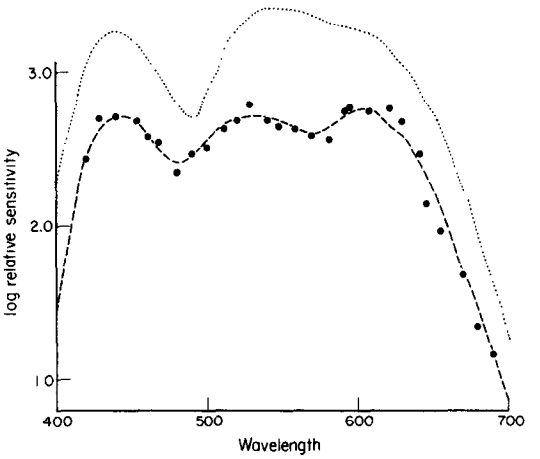

Fig. 5. The white-adapted spectral sensitivity at suprathreshold (---) from equations (3) using differential (adapting) weights to depress V_λ and $+y$, compared to Sperling and Harwerth (1971) (●). The dotted curve, which has been displaced upward, shows the spectral sensitivity from equations (3) using no differential weights.

requires adjustment of the coefficients. For the lower dashed curve, the coefficients have been adjusted to fit data for one of Sperling and Harwerth's (1971) subjects. This data was obtained from rhesus macaques by measuring increment thresholds to spectral lights upon intense white backgrounds. Although Sperling and Harwerth modeled their curves by using pieces of r–g opponent curves and an S pigment curve, which implies that their white adaptation essentially removed any V_λ and $+y$ contribution (V_λ and $+y$ have similar spectral sensitivities), equation (1) gives a good fit to the empirical points if the y–b and V_λ channels are only attenuated about one-half by the adaptation. The coefficients used for the fit shown are: $(r\text{–}g)^* = 1.2\,L - 1.4\,M + 0.07\,S$; $(y\text{–}b)^* = 0.4\ (y\text{–}b)$ and $V_\lambda^* = 0.4\ (V_\lambda)$.

Additional macular pigment (0.34 density at 460 nm) was also added for the monkey eye.

None of the above spectral sensitivities yield additive luminances because of the opponent terms in equation (1). They therefore agree with the general findings of subadditivity for those sensitivity measures which do not exclude brightness contributions from the opponent channels. Two measures of spectral sensitivity which assign additive relative brightness to different wavelengths are flicker photometry and direct comparison by minimizing the distinctness of a border (e.g. see Wagner and Boynton, 1972). The features required to produce additive luminances were incorporated in the model by assigning different temporal and spatial properties to the axes in the vector space. Thus the phasic cells on the V_λ axis resolve flicker to higher frequencies than the tonic cells lying in the chromatic plane. Consequently, experiments which use a flicker criterion will isolate the spectral sensitivity of this axis. The other axes add brightness and hue to the flicker fields, but this brightness does not help resolve the flicker and thus does not add to the sensitivity. The spatial properties of the receptive fields account for the additivity of minimum-border matches on the assumption that borders are minimized by eliminating what is sometimes called the contrast enhancement produced by reciprocal lateral inhibition occurring at the border. Such re-

sponses are produced only by the receptive fields of the achromatic channel to a minimum-border stimulus [e.g. see Fig. 2 of Ingling and Drum (1973)].

THE STRUCTURE OF STILES'S π_5 MECHANISM

The above four kinds of spectral sensitivity—absolute threshold, white adapted, flicker and minimum-border—do not involve chromatic adaptations, and hence no alterations in the shape of the opponent or V_λ curves. Spectral sensitivity curves measured for states of adaptation other than neutral require adjustment of the coefficients of the transformation equations [equations (2) and (3)] as well as adding coefficients before the channel sensitivities of equation (1). This applies in particular to the derivation of the shapes of spectral sensitivity curves isolated by both Stiles's test and field sensitivity methods. The former measures the sensitivity as a function of wavelength to test lights superimposed upon a fixed chromatic background; the latter measures the radiance of spectral backgrounds required to give a criterion elevation of a fixed-wavelength test flash. The reciprocals of the background radiances against wavelength are taken to be the spectral sensitivity of the mechanism which detects the fixed test flash. To a first approximation, within-term chromatic adaptation effects can be ignored compared to the effect upon the between-term coefficients, although to do so introduces error in the sensitivity curve.

For, say, the π_5 field sensitivity to be the spectral sensitivity of the L cones, at least these two assumptions must be met: (i) The fixed test flash must be detected by only the L cones; and (ii) the variable background used to raise the threshold of the L cones must do so only because of quantum absorptions in the L cones themselves. In other words, the mechanisms must be independent. Quantum absorptions in the S and M cones must not change the effective sensitivity of the L cones. From equations (1)–(3), the first two terms of course show that quantum absorptions in M cones do change the effective sensitivity of L cones. (By the term "effective sensitivity" it is meant that at some stage the output of M cones inhibits the output of L cones, not necessarily that one cone directly alters the sensitivity of another.) Thus, the independence assumption is not met for the conditions under which π mechanisms are measured (e.g. see Boynton, Ikeda and Stiles, 1964). A rigorous derivation using equation (1) would use interterm coefficients as noted above, but an approximation illustrates the effect of failing to meet the independence assumption.

The independence assumption (ii) can be satisfied by flickering the increment upon the background and requiring the observer to detect the flicker instead of the increment. Flicker eliminates the first two terms of equation (1), thus restoring independence. If the first assumption, that only L cones detect the test flash, is met, then the radiance of the backgrounds must be inversely proportional to the sensitivity of the L cone to bring the flickering test to threshold at each background wavelength.

If the test increment is not flickered upon the background, then there will be a contribution from the first two terms. This contribution is depressed relative to the achromatic V_λ term because of the chromatic adaptation, since each threshold is measured upon a spectral background. This is analogous to the depression of the V_λ sensitivity by white adaptation. In addition to the reduction of the chromatic channels relative to the achromatic, the adapting backgrounds have unequal effects upon the two chromatic channels; adaptation reduces the sensitivity of the y–b more than the r–g. Stiles (1953) reports that the Weber fraction for π_1, a short-wavelength mechanism, is five times that of the longer wavelength mechanisms. That is, adapting lights increase the threshold five times more for the system fed by the S cones than for the other cone systems. To model this effect, let the backgrounds used to measure the field sensitivity depress the sensitivity of the y–b and r–g channels in the ratio of 5:1. Reducing the opponent channel sensitivity by 0.49, an empirical estimate of the relative loss of chromatic channel sensitivity caused by chromatic adaptation, gives the following expression for π_5, plotted in Fig. 6 (top):

$$S^2 = Q^2\{0.49\,[(r\text{–}g)^2 + 1/5\,(y\text{–}b)^2] + (0.6L + 0.4M)^2\}, M = 0. \quad (4)$$

Another way of looking at this model is to note that π_5 is the spectral sensitivity of L with a weighted intrusion of brightness from the chromatic channels,

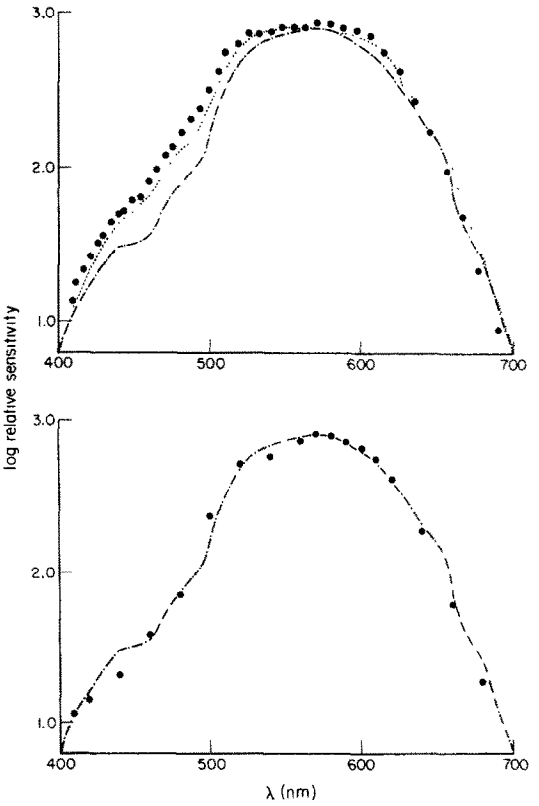

Fig. 6. Top: comparison of Stiles's π_5(···), the L fundamental sensitivity (·—·—·) and the vector model of π_5 (·····). Bottom: comparison of σ_5 (the reciprocal of the radiance of a 10° background required to raise a 1° 10-Hz square-wave flickering increment 5× (more usually 10×) above the absolute flicker threshold) with the L sensitivity.

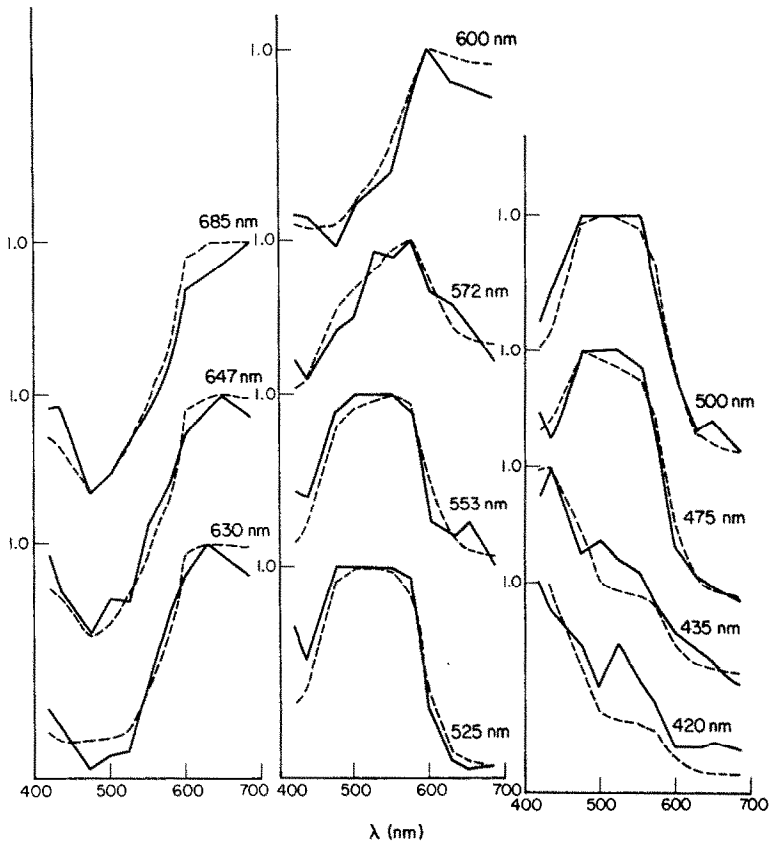

Fig. 7. A comparison of Guth *et al.*'s (1969) threshold additivity functions (——) with the predictions of the vector space of (---) Figs. 1 and 2.

which the use of a flicker criterion removes. Figure 6 illustrates the theoretical and empirical functions.[1] Calculated or measured field sensitivities for which detection of 10-Hz square-wave flicker was the criterion, rather than detection of a test flash, are called σ mechanisms to distinguish them from π mechanisms. In view of the widespread use of Stiles's field sensitivity method, we emphasize that detection of flicker in an increment appears more valid than detection of the increment if it is desirable to satisfy the assumption of independence.

OTHER DISCRIMINATION FUNCTIONS

Figure 7 shows our vector model predictions [equation (2)] with Guth, Donley and Marrocco's (1969) empirical data on the additivity of mixtures of lights at threshold. Guth *et al.* determined the threshold for, say, a green light and a red light, and then found the amount of the green light in threshold units that must be added to half a threshold unit of red light to reach threshold. Such mixtures are subadditive; more than half—say, 0.75 of a threshold unit of green light is required for threshold when mixed with the 0.5 red. Hence, the magnitudes do not add as scalar quantities, but may add as vectors. Choose an angle between the 0.75 green and the 0.5 red such that their resultant is 1.0 threshold unit. The ordinates of Fig. 7 show the cosines of the angles required between the wavelength which labels each curve and the wavelengths on the abscissa which are mixed with it. These cosines are calculated in the threshold vector space; the measured cosines are also shown.

Figure 8 (bottom) compares the theoretical saturation discrimination function with typical empirical functions. The saturation discrimination functions are measured by determining the least amount of spectral light which must be added to a white light to make it just noticeably different from a comparison light. The brightness of the mixture is kept equal to the comparison field during the mixing so that the discrimination is made on the hue. The discrimination function is a plot of the logarithm of the reciprocal of the colorimetric purity of the mixture against the wavelength of the added spectral light. To derive this function in the vector space, let L_c be the luminance of the spectral component and L_w be the luminance

[1] This experiment will be reported fully elsewhere. The procedure for measuring a σ mechanism is identical to that for measuring a π mechanism, with the sole exception that the subject is instructed to adjust the 1° 10 Hz flickering test until the flicker, and not the increment itself, is at threshold upon the background. Spectral sensitivity curves are derived by first measuring flicker-threshold vs background radiance curves (ftvr curves), noting the radiance which produces a criterion elevation of the flicker threshold, and finally plotting the reciprocals of these radiances against wavelength.

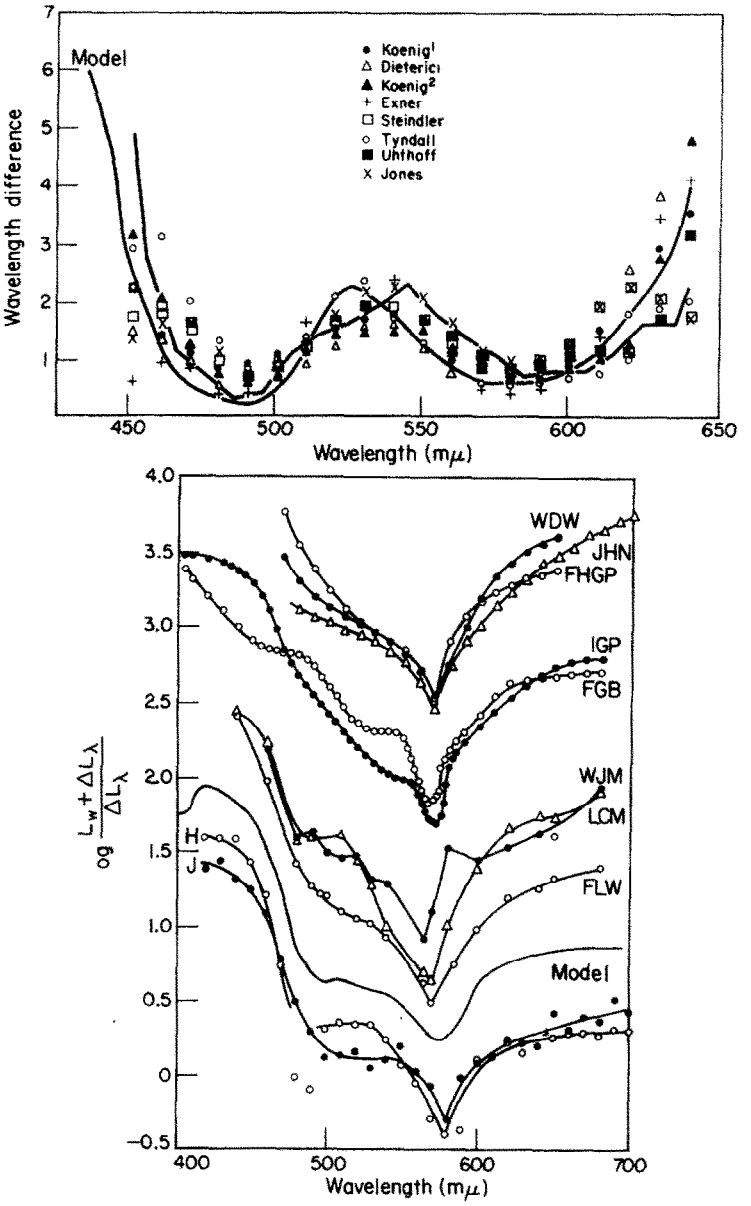

Fig. 8. A comparison of the saturation and wavelength discrimination curves from the vector space with empirical functions from Jameson and Hurvich (1955) and Judd (1932), respectively.

of the white component. Then $L_c + L_w = K$, the constant luminance of the comparison side.

$$\text{Colorimetric purity} = \frac{L_c}{L_w + L_c} = \text{cp}$$

$$\log \frac{1}{\text{cp}} = \log \frac{L_w + L_c}{L_c} = \log \frac{K}{L_c}$$

$$= \log \frac{K}{\text{chromatic luminance required for criterion response}}$$

$$= \log \frac{K}{V_\lambda \text{ chromatic radiance required for criterion response}}$$

$$= \log \frac{K(\text{chromatic spectral sensitivity})}{V_\lambda}$$

$$= \log \left\{ \frac{K\sqrt{[(r-g)^2 + (y-b)^2]}}{V_\lambda} \right\}.$$

The above expression produces the theoretical curve plotted in Fig. 8 (bottom).

Figure 8 (top) compares the wavelength discrimination function of the vector space with a survey of those in the literature. The wavelength discrimination function is measured by finding a $\Delta\lambda$ which makes one side of a spectral field just noticeably different from the other. This corresponds, in the vector space, to finding the $\Delta\lambda$ required to produce a criterion angular displacement of an origin-bound vector.

DISCUSSION AND CONCLUSIONS

From the illustrations given, a simple vector space using opponent and luminances axes provides a useful approximate theory for foveal color vision of aperture colors. The theory is simple enough to use in estimating the outcome of many color vision experiments, although exact parameters must be determined by experiment. At present, the model is limited by insufficient knowledge of how the channel sensitivities change as a function of intensity and adaptation.

Acknowledgement—Research partially supported by NIH Grant No. R01-EY00148 to Carl R. Ingling, Jr.

REFERENCES

Boynton R. M., Ikeda M. and Stiles W. S. (1964) Interactions among chromatic mechanisms as inferred from positive and negative increment thresholds. *Vision Res.* **4,** 87–117.

Dagher M., Cruz A. and Plaza L. (1958) Colour thresholds with monochromatic stimuli in the spectral region 530–630 nm. In *Visual Problems of Colour* I, p. 319. N.P.L. Symp. No. 8. H.M.S.O., London.

DeValois R. L., Abramov I. and Jacobs G. H. (1966) Analysis of response patterns of LGN cells. *J. opt. Soc. Am.* **56,** 966–977.

Gouras P. (1968) Identification of cone mechanisms in monkey ganglion cells. *J. Physiol., Lond.* **199,** 533–575.

Guth S. L., Donley N. J. and Marrocco R. T. (1969) On luminance additivity and related topics. *Vision Res.* **9,** 537–575.

Guth S. L. and Lodge H. R. (1973) Heterochromatic additivity, foveal spectral sensitivity, and a new color model. *J. opt. Soc. Am.* **63,** 450–462.

Hsia Y. and Graham C. H. (1957) Spectral luminosity curves of protanopic, deuteranopic, and normal subjects. *Proc. natn. Acad. Sci. U.S.A.* **43,** 1011–1019.

Ingling C. R., Jr. (1977) The spectral sensitivity of the opponent-color channels. *Vision Res.*, In press.

Ingling C. R., Jr. and Drum B. A. (1973) Retinal receptive fields: correlations between psychophysics and electrophysiology. *Vision Res.* **13,** 1151–1163.

Ingling C. R., Jr., Tsou B. H-P. and Nosek T. (1973) A transformation of color space with photometric properties. Paper presented at ARVO Spring Meeting, May, 1973.

Jacobs G. H. and Wascher T. C. (1967) Bezold–Brücke hue shift: further measurements. *J. opt. Soc. Am.* **57,** 1155–1156.

Jameson D. and Hurvich L. M. (1955) Some quantitative aspects of an opponent-colors theory. I. Chromatic responses and spectral saturation. *J. opt. Soc. Am.* **45,** 546–552.

Judd D. B. (1932) Chromaticity sensibility to stimulus differences. *J. opt. Soc. Am.* **22,** 72–108.

Judd D. B. (1951) Basic correlates of the visual stimulus. In *Handbook of Experimental Psychology* (Edited by Stevens S. S.). Wiley, New York.

Kaiser P. K., Herzberg P. A. and Boynton R. M. (1971) Chromatic border distinctness and its relation to saturation. *Vision Res.* **11,** 953–968.

Richards W. (1967) Differences among color normals: Classes I and II. *J. opt. Soc. Am.* **57,** 1047–1055.

Smith V. C. and Pokorny J. (1975) Spectral sensitivity of the foveal cone photopigments between 400 and 500 nm. *Vision Res.* **15,** 161–171.

Sperling H. G. and Harwerth R. S. (1971) Red-green cone interactions in the increment-threshold spectral sensitivity of primates. *Science* **172,** 180–184.

Stiles W. S. (1953) Further studies of visual mechanisms by the two-colour threshold method. *Coloquio sobre problemas opticos de la vision*, Madrid. **1,** 65, 103. Union Internationale de Physique Pure et Appliquée.

Vos J. J. and Walraven P. L. (1971) On the derivation of the foveal receptor primaries. *Vision Res.* **11,** 799–818.

Wagner G. and Boynton R. M. (1972) Comparison of four methods of heterochromatic photometry. *J. opt. Soc. Am.* **62,** 1508–1515.

Wiesel T. N. and Hubel D. H. (1966) Spatial and chromatic interactions in the lateral geniculate body of the rhesus monkey. *J. Neurophysiol.* **29,** 1115–1156.

Wyszecki G. and Stiles W. S. (1967) *Color Science.* Wiley, New York.

APPENDIX: TRANSFORMATION FOR VOS AND WALRAVEN'S RGB TO OPPONENT SPECTRAL SENSITIVITIES

With the differences discussed below, the following equations are the counterparts for Vos and Walraven's RGB fundamentals of equations (2)–(4), respectively.
The threshold equations:

$$r\text{–}g = 2R\text{–}4G$$
$$y\text{–}b = K(0.4R + 0.3G - 70B),\ K = 0.115$$
$$V_\lambda = R + G + B.$$

The suprathreshold equations:

$$r\text{–}g = 2R - 4G + 39B$$
$$y\text{–}b = K(0.4R + 0.3G - 70B),\ K = 1$$
$$V_\lambda = R + G + B.$$

The above two sets of equations may be reduced to the single set:

$$r\text{–}g = -(-2R + 4G\ \theta\ 39B)$$
$$y\text{–}b = K(0.4R + 0.3G - 70B).$$

There are significant differences between the transformation equations for RGB and those for LMS: (i) RGB are normalized to sum to Judd's modified $\bar{y}$ (Wyszecki and Stiles, 1967, p. 436). LMS are normalized to 1.00 at λ_{max}. (ii) According to Vos and Walraven, V_λ receives input from all three types of cone, R, G and B; but for the Pokorny's V_λ, only the L and M cones contribute. The question of blue cone input to the achromatic channel cannot be answered on the basis of these models. Recent proposals favor the L and M model. Guth (1969) proposed that V_λ lacked blue cone input, a suggestion pursued by Smith and Pokorny (1975) and also supported by Gouras (1968) who found no blue-cone input to phasic units. (iii) For the y–b channel, the RGB equations follow a different principle than the LMS equations. For the former, the suprathreshold y–b sensitivity is obtained from the threshold by multiplying by a constant, following Judd (1951). To a first approximation, this accounts for the Bezold–Brücke effect, which is that yellows and blues grow with intensity faster than reds and greens. It also requires that unique green, the hue identified with the crosspoint of the y–b sensitivity curve, remain fixed at all intensities. The literature, a review of which is beyond the scope of this report, disagrees about the invariance of unique green. However, Fig. 9 shows evidence from three studies supporting a shift

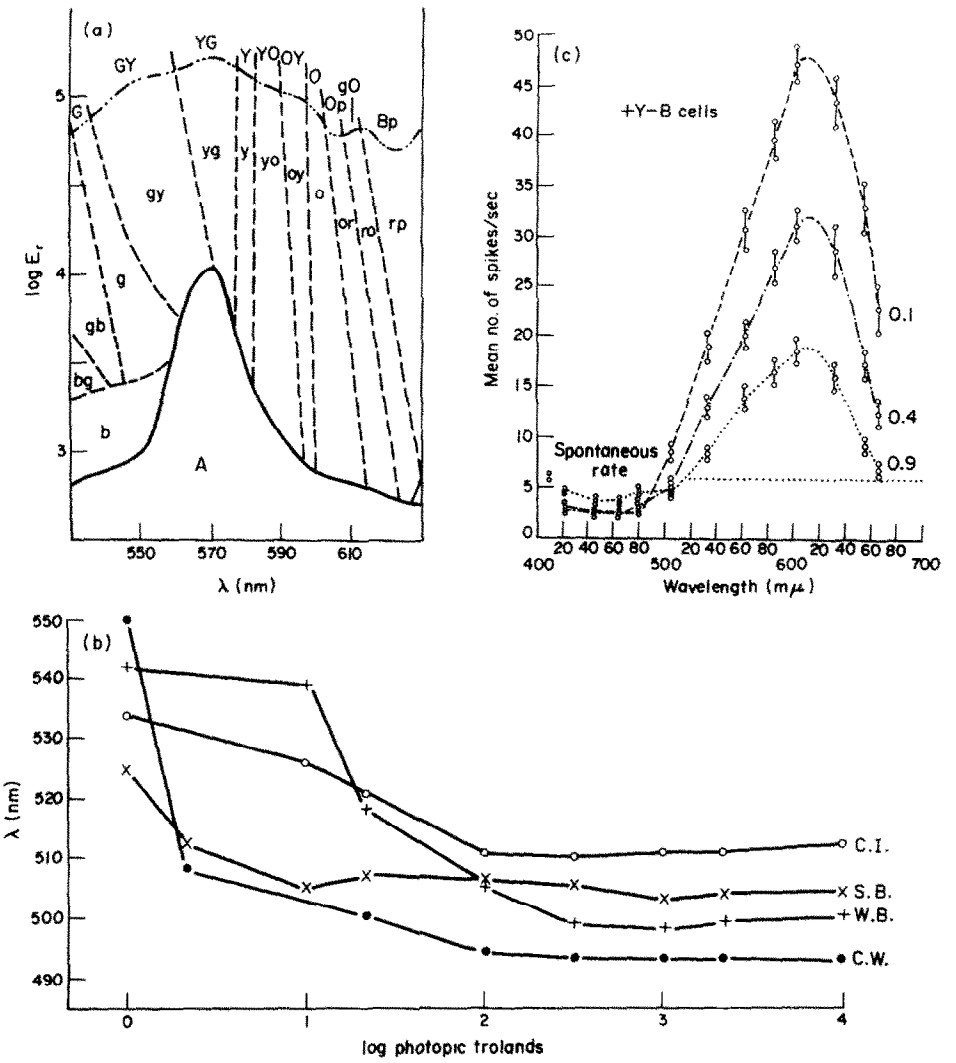

Fig. 9. (a) Lines of constant hue as a function of intensity from Dagher *et al.* (1958). (b) Variation with intensity of spectral locus of the hue identified as unique green; 1° foveal 0.5-sec flashes (c) LGN recordings from y–b cells as a function of intensity (from DeValois *et al.*, 1966). The crosspoint, which is presumably the locus of unique green, shifts toward shorter wavelengths with increasing intensity.

toward shorter wavelengths with intensity. Figure 9(a) shows lines of constant hue as a function of intensity from Dagher, Cruz and Plaza (1958), 9(b) confirming data that we have obtained[2] and 9(c) LGN recordings from y–b cells as a function of intensity by DeValois, Abramov and Jacobs (1966). Finally, Jacobs and Wascher (1967) report a similar shift, and also note that such a shift is consistent with the results of DeValois *et al.*

These data are inconsistent with Judd's simple model used with the RGB transformation. The LMS equations for the y–b channel move the crosspoint to shorter wavelengths with increasing intensity. Because some subjects have unique green at very long wavelengths, the channel sensitivity at low intensities must be largely y–M, becoming y–S at high intensities. Apparently, the M input does not increase as rapidly with intensity as does the S. At low intensities the S contribution to what is essentially a y – (S + M) channel is small compared to M; at high intensities M is small compared to S. Figure 9 shows the shift of the y–b crosspoint to shorter wavelengths. In effect, Judd's Bezold–Brücke factor applies only to the S component of the short-wavelength input to the y–b channel. (Fig. 1, intended to illustrate the suprathreshold case, omits the low-intensity M-cone signal to the y – (S + M) channel.)

[2] This experiment will be reported fully elsewhere. The data shown were obtained for ½-sec flashes presented once every 4 sec. The stimulus subtended 1.25° of visual angle. The psychophysical method was a forced staircase; the subject pushed a button signaling blue or yellow, which automatically lengthened or shortened, respectively, the 10 td for dark-adapted conditions and long interstimulus intervals unique green remains constant with intensity. Below 10 td the wavelength of the hue perceived as neither bluish nor yellowish tends to move toward longer wavelengths. For some subjects [Class II: Richards (1967)] the shift to longer wavelengths occurs at higher intensities, particularly, if the subject is not carefully dark-adapted.
stimulus wavelength. The experimenter occasionally reversed the direction to control for undesirable strategies which the subject might adopt. Roughly speaking, above